Critical dynamics and global persistence in a probabilistic three-states cellular automaton

Roberto da Silva (corresponding author)*

Departamento de Informática Teórica, Instituto de Informática,

Universidade Federal do Rio Grande do Sul.

Av. Bento Gonçalves, 9500, CEP 90570-051 Porto Alegre RS Brazil

Nelson Alves Junior†

Departamento de Física e Matemática, Faculdade de Filosofia,

Ciências e Letras, Universidade de São Paulo.

Av. Bandeirantes, 3900-CEP 014040-901 Ribeirão Preto SP Brazil

Abstract

In this work a three-states cellular automaton proposed to describe part of a biological immune system [6] is revisited. We obtain the dynamic critical exponent z of the model by means of a recent technique that mixes different initial conditions. Moreover, by using two distinct approaches, we have also calculated the global persistence exponent θ_g, related to the probability that the order parameter of the model does not change its sign up to time t $[P(t) \propto t^{-\theta_g}]$.

*Electronic address: rdasilva@inf.ufrgs.br

†Electronic address: nalves@dfm.ffclrp.usp.br

I. INTRODUCTION

Cellular automata are statistical-mechanical models which present a complex behavior, despite their relatively simple dynamic rules. In general these models are defined in d-dimensional lattices with linear dimension L, in which each site i $(1 \leq i \leq L^d)$ is occupied by a variable s_i. The dynamic rules of a typical cellular automaton have two basic characteristics: Firstly, the update of a variable s_i depends only on its neighborhood (short-range interactions). Secondly, given a configuration of the system at instant t, at instant $t+1$ all variables s_i $(1 \leq i \leq L^d)$ are updated at once. The use of cellular automata in order to mimic biological immune systems has improved the understanding about the microscopic mechanisms that lead to the macroscopic behavior of these systems [1]. For example, cellular automata are as usefull to describe the T-helper cells response under parasitic infections [2, 3] as they are to model the course of the Human Immunodeficiency Virus (HIV) infection [4].

Brass *et al.* divised a simple cellular automaton model of $\mathrm{T_H}$ cell interactions to mimic the immune system of mice exposed to parasitic infections [2, 3]. The model is defined in a cubic $(d = 3)$ lattice in which each site is occupied by one of three different $\mathrm{T_H}$ cell types: $\mathrm{T_H}0$, $\mathrm{T_H}1$ and $\mathrm{T_H}2$ cells. T-helper cells that have not yet been presented to the antigen are denoted by $\mathrm{T_H}0$. In the model, two distinct routes (equivalent to two populations of antigen presenting cells) govern the maturing of a $\mathrm{T_H}0$ cell: Antigen presented by the first (second) route elicit a $\mathrm{T_H}1$ ($\mathrm{T_H}2$) response. In order to take into account the competition between mature $\mathrm{T_H}$ cells, the induction $\mathrm{T_H}0 \rightarrow \mathrm{T_H}1$ ($\mathrm{T_H}2$) is forbidden when the neighborhood of the $\mathrm{T_H}0$ cell has an overall majority of $\mathrm{T_H}2$ ($\mathrm{T_H}1$) cells. At last, a mature cell dies (it is substituted by a $\mathrm{T_H}0$ cell) if such a cell is not restimulated by the appropriate antigen within the time interval N_T. The model can display a spontaneous symmetry breaking as one varies the antigen density or the cutoff N_T, in agreement with experimental results [5]. A probabilistic version of the model was proposed by Tomé and Drugowich de Felício [6] by allowing the death of cells $\mathrm{T_H}1$ and $\mathrm{T_H}2$ at each time step with a probability r. Thus, in this modified version of the model, the lifetime N_T was substituted by a mean lifetime related to the probability r. Also, the development of $\mathrm{T_H}0$ cells into either $\mathrm{T_H}1$ or $\mathrm{T_H}2$ cells occurs with a probability that depends on the neghborhood of the $\mathrm{T_H}0$ cell and on a parameter p, related to the antigen density. Such probabilistic version presents the intrinsic spontaneous symmetry breaking found in the Brass *et al.* automaton, besides being amenable to an analytical approach [6]. The critical behavior of the probabilistic model proposed in Ref. [6] was studied in a subsequent work by Ortega *et al.* [7]. By using a finite-size scaling analysis, from Monte Carlo simulations of square lattices, Ortega *et al.* determined the ratios of exponents $\frac{\beta}{\nu}$ and $\frac{\gamma}{\nu}$, as well as the critical point of the

model. Their results suggest that the probabilistic automaton, although not satisfying detailed balance, belongs to the same universality class of the two-dimensional kinetic Ising model [7], thus supporting the *up-down* conjecture, introduced by Grinstein *et al.* [8]. In a subsequent work, Tomé and Drugowich [9] obtained the dynamic critical exponent z of the probabilistic automaton in two dimensions, by performing short-time Monte Carlo simulations by studying the collapse of the fourth order Binder's cumulant for different lattice sizes.

In the present work we have revisited the probabilistic automaton of Ref. [6]. We have re-obtained the dynamic critical exponent z of the automaton by using a recent technique that mixes different initial conditions [10]. Such technique is based upon the short-time critical dynamics introduced by Janssen *et al.* [11], who showed that even far from equilibrium the short-time relaxation of the order parameter follows a universal scale form

$$M(t) = m_0 t^{\theta}, \tag{1}$$

where $M(t)$ is the order parameter at instant t (measured in Monte Carlo steps per Spin - MCS), $m_0 = M(0)$ is a small initial ($t = 0$) value of the order parameter, and θ is the dynamic critical exponent, related to the increasing of the order parameter after the quenching of the system (When dealing with Monte Carlo simulations, the time t is discrete and measured in Monte Carlo Steps per Spin - MCS). Eq. (1) demands working with sharply prepared initial states with a precise value of m_0. After obtaining the critical exponent θ for a number of m_0 values, the final value for θ is obtained from the limit $m_0 \to 0$.

Starting from an ordered state ($m_0 = 1$), the order parameter $M(t)$ decays in time, at the critical temperature, according to the power law [12]

$$\langle M(t) \rangle_{m_0=1} \sim t^{-\beta/\nu z}, \tag{2}$$

where $\langle(\cdots)\rangle$ is the average of the quantity $(\cdots)$ over different samples with initial order parameter value $m_0 = M(0)$, β and ν are the usual static critical exponents, related to the order parameter and to the correlation length, respectively, and z is the dynamic critical exponent, defined as $\tau \sim \xi^z$, where τ and ξ are time and spatial correlation lengths, respectively.

Starting from a disordered configuration with $m_0 = 0$, the second moment of the order parameter increases after the power law

$$\langle M^2(t) \rangle_{m_0=0} \sim t^{\omega}, \tag{3}$$

where the exponent ω is given by

$$\omega = \left(d - \frac{2\beta}{\nu} \right) \frac{1}{z}, \tag{4}$$

and d is the dimension of the system.

By combining Eqs. (2) and (3), da Silva *et al.* [10] obtained the ratio

$$F_2 = \frac{\langle M(t)^2 \rangle_{m_0=0}}{\langle M(t) \rangle^2_{m_0=1}} \sim t^{d/z}, \tag{5}$$

which corresponds to a function with mixed initial conditions. At this point, it is important to stress here that, from Eq. (5) above, two independent runs are necessary in order to calculate the ratio F_2: In one of them $m_0 = 0$ (numerator), while in the other one $m_0 = 1$ (denominator). The ratio F_2 has proven to be useful in determining the exponent z, according to recent studies of the 2D Ising model [10], $q = 3$ and $q = 4$ states Potts models [10], Ising model with next-nearest-neighbor interactions [13], Baxter-Wu model [14], at the tricritical point of the 2D Blume-Capel model [15], at the Lifshitz point of the 3D ANNNI model [16] and in other studies concerning models with one absorbent state [17].

In addition, in this work we have also calculated the global persistence exponent θ_g [18], related to the probability that the order parameter of the model, $M(t)$, does not change its sign up to time t, after a quench of the system to the critical temperature.

The layout of this paper is as follows: In section II we explain the model. In section III we define the order parameter $M(t)$ and we describe the methodology used in order to obtain the dynamic critical exponents θ_g and z. In section IV the results obtained for the exponents z and θ_g are shown. Finally, in section V we present the main concluding remarks.

II. THE MODEL

In this work we have studied a two-dimensional probabilistic cellular automaton in which dynamics is governed by local stochastic rules. At each site i of the square lattice we have attached a variable σ_i assuming the value $0, +1$ or -1, depending on whether the site is occupied by a $\mathrm{T_H}0$, a $\mathrm{T_H}1$ or a $\mathrm{T_H}2$ cell, respectively. Considering N the total number of sites in the lattice, we have defined the set $\sigma = (\sigma_1, \sigma_2, \cdots, \sigma_N)$ to represent the microscopic state of the system.

The probability of state σ at time t, $P_t(\sigma)$, evolves in time according to the equation

$$P_{t+1}(\sigma') = \sum_{\sigma} W(\sigma'|\sigma) P_t(\sigma), \tag{6}$$

where the transition probability $W(\sigma'|\sigma)$ from state σ to state σ' obeys the condition

$$\sum_{\sigma'} W(\sigma'|\sigma) = 1. \tag{7}$$

On the other hand, for a system that evolves at discrete time steps, in which all the sites are updated at once, as is the case for the cellular automaton in this work, the transition probability $W(\sigma'|\sigma)$ is written in the form

$$W(\sigma'|\sigma) = \prod_{i=1}^{N} \omega_i(\sigma'_i|\sigma), \tag{8}$$

where $\omega_i(\sigma'_i|\sigma)$ is the conditional probability that site i be in the state σ'_i at time $t+1$, given that the state of the system is σ at instant t. Such conditional probability satisfies the condition

$$\sum_{\sigma'_i} \omega_i(\sigma'_i|\sigma) = 1, \tag{9}$$

what implies immediately that Eq. (7) is fulfilled. The cellular automaton investigated in this work belongs to the class of totalistic cellular automata [19]. Thus, the transition probability $\omega_i(\sigma'_i|\sigma)$ depends on σ_i and on the sum $\xi = \sum_\delta \sigma_{i+\delta}$, where the sum runs over the neighborhood of site i. More specifically, we are considering a particular kind of totalistic automaton for which $\omega_i(\sigma'_i|\sigma)$ depends only on the sign of the sum ξ. By defining

$$s_i = \mathrm{sign}(\xi) = \begin{cases} 1 & \text{if } \xi > 0, \\ 0 & \text{if } \xi = 0, \\ -1 & \text{if } \xi < 0, \end{cases} \tag{10}$$

we may use the notation $\omega_i(\sigma'_i|\sigma_i, s_i)$ in order to explicit the transition probability dependence on σ_i and s_i.

The transition probabilities (dynamical rules) are given by

$$\omega_i(+1|\sigma_i, s_i) = p\delta(\sigma_i, 0)\{\delta(s_i, +1) + \frac{1}{2}\delta(s_i, 0)\} + (1-r)\delta(\sigma_i, +1), \tag{11}$$

$$\omega_i(-1|\sigma_i, s_i) = p\delta(\sigma_i, 0)\{\delta(s_i, -1) + \frac{1}{2}\delta(s_i, 0)\} + (1-r)\delta(\sigma_i, -1), \tag{12}$$

$$\omega_i(0|\sigma_i, s_i) = (1-p)\delta(\sigma_i, 0) + r\{\delta(\sigma_i, +1) + \delta(\sigma_i, -1)\}, \tag{13}$$

where, as discussed in section I, r is the death probability of T_H1 and T_H2 cells, and p is a parameter related to the antigen density [6].

The dynamical rules (11), (12) and (13) above have "up-down", *i.e.*,

$$\omega_i(\sigma'_i|\sigma_i, s_i) = \omega_i(-\sigma'_i| - \sigma_i, -s_i). \tag{14}$$

Therefore, following Grinstein *et al.* [8], we expect that the probabilistic cellular automaton investigated in this work be at the same universality class of kinetic Ising models.

III. THE ORDER PARAMETER AND THE DYNAMIC EXPONENT θ_g

A. Order parameter

In the short-time Monte Carlo simulations performed in this work the order parameter $M(t)$, as well as its higher moments $M^{(k)}(t)$, were obtained from averages over a certain number of samples, N_s. By defining the kth momentum of the order parameter in sample number j at instant t as

$$M_j^k(t) = \frac{1}{L^{2k}} \left(\sum_{i=1}^{L^2} \sigma_{ij}(t) \right)^k , \tag{15}$$

the order parameter is written in the form

$$M^{(k)}(t) = \left\langle M_j^k(t) \right\rangle = \frac{1}{N_s L^{2k}} \sum_{j=1}^{N_s} \left(\sum_{i=1}^{L^2} \sigma_{ij}(t) \right)^k . \tag{16}$$

As defined in Eqs. (15) and (16) above, for $k = 1$ the order parameter is exactly the mean magnetization, $M^{(1)}(t) = \langle M(t) \rangle$.

Eq. (16) defines the order parameter and its higher moments for a set of N_s samples. Thus, if N_b sets of samples are considered at instant t, there are N_b measurements of the magnetization (and its higher moments), $M_l^{(k)}(t)$, where $1 \leq l \leq N_b$. By considering such sets of samples, the final value of the magnetization and its higher moments are obtained from the average over the N_b sets of samples, *i.e.*,

$$\overline{M^{(k)}}(t) = (1/N_b) \sum_{l=1}^{N_b} M_l^{(k)}(t), \tag{17}$$

where $M_l^{(k)}(t)$ is given by Eq. (16) and the corresponding standard deviation is given by

$$\sigma \left[M_l^{(k)}(t) \right] = \frac{1}{\sqrt{N_b(N_b - 1)^2}} \left(\sum_{l=1}^{N_b} \left(M_l^{(k)}(t) - \overline{M^{(k)}}(t) \right)^2 \right)^{1/2} . \tag{18}$$

B. Dynamic critical exponent θ_g

In this section we define the dynamic critical exponent θ_g and we describe two methods used in this work to obtain estimates for θ_g.

In the first method , we have performed short-time Monte Carlo simulations in order to calculate the global persistence probability $P(t)$, *i.e.*, the probability that the magnetization does not change its sign up to time t. On the other hand, the probability $P(t)$ is numerically equal

to the complement of the accumulated distribution $p(t)$, according to which the magnetization changes its sign for the first time exactly at instant t, *i.e.*,

$$P(t) = 1 - \sum_{t'=1}^{t} p(t') = 1 - \sum_{t'=1}^{t} \frac{n(t')}{N_s}, \tag{19}$$

where $n(t')$ is the number of samples for which the magnetization changes its sign for the first time at instant t' and N_s is the total number of samples. The exponent θ_g may be obtained directly from the power law scale relation [18]

$$P(t) \sim t^{-\theta_g}, \tag{20}$$

from which we obtain $\ln P(t) = c - \theta_g \ln t$, where c is constant and each run requires a sharply prepared initial state, with a precise small value of m_0, as discussed in Eq. (1).

In a second way to obtain the exponent θ_g we have used the fact that the initial magnetization dependence of $P(t)$ can be cast in the following finite-size scaling relation [18],

$$P(t) = t^{-\theta_g} f(t/L^z) = L^{-\theta_g z} \tilde{f}(t/L^z)\,, \tag{21}$$

which renders a different method to obtain the exponent θ_g from lattice sizes L_1 and L_2 [18]. For this end we define $W(t, L) = L^{\theta_g z} P(t)$, which turns out to be a function of t/L^z. Therefore, if we fix the dynamic exponent z, the exponent θ_g can be obtained by collapsing the time series $W(t_2, L_2) = f(t_2/L_2^z)$ onto $W(t_1, L_1) = f(t_1/L_1^z)$ as follows. Under re-scaling, with $b = L_2/L_1$, $(L_2 > L_1)$, we obtain

$$W(t_2, L_2) = \widetilde{W}(b^z t_1, bL_1)\ , \tag{22}$$

and the best estimate for θ_g corresponds to the minimization of

$$\chi^2(\theta_g) = \sum_t \left(\frac{W(t, L) - \widetilde{W}(b^z t, bL)}{|W(t, L)| + \left|\widetilde{W}(b^z t, bL)\right|} \right)^2 \tag{23}$$

by interpolating $\widetilde{W}$ to the time values $b^z t$. In order to obtain the exponent θ_g using the collapse method described above, it is not necessary to fix a precise value of the initial magnetization m_0 in the short-time simulations, once the scaling relation in Eq. (21) does not take into account the initial conditions of the system. So, we have used initial states in which $\langle m_0 \rangle \sim 0$. On the other hand, the collapse method demands the dynamic exponent z to be known beforehand. Therefore, in this work we have used the scaling relation of Eq. (5) in order to obtain estimates for the exponent z. Although both methods described by Eqs. (20) and (21) were proposed in order to calculate the exponent θ_g of the two-dimensional Ising model [18], such methods were used recently for estimates of θ_g along the critical line and at the tricritical point of the 2D Blume-Capel model [20].

IV. RESULTS FROM SHORT-TIME MONTE CARLO SIMULATIONS

In this section we present details about the short-time Monte Carlo simulations performed for the cellular automaton considered in this work, as well as the results obtained for both dynamic critical exponents z and θ_g.

A. Critical parameters

Initially we refine the critical parameter $r = 0.196$ obtained in Ref. [6]) for $p = 0.3$. From Eq. (2) we expected a straight line for the log-log plot of $M(t)$ against t at the critical point ($p = 0.3; r = 0.196$). However, from log-log plots of Eq. (2) obtained for different values of r, we observed that more accurate straight lines are obtained for $r \neq 0.196$, as depicted in Fig. 1 for $r = 0.190, 0.192, 0.194, 0.196$ and 0.198. In the short-time simulations performed in order to obtain the curves shown in Fig 1 we have used square lattices ($d = 2$) with linear dimensions $L = 160$, $N_s = 10000$ samples, $N_b = 5$ sets of samples and 1000 MCS. For each value of r used

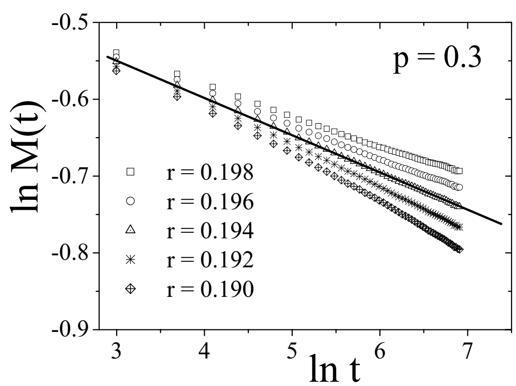

FIG. 1: Log-log plots of the order parameter (magnetization) $M(t)$ versus t, constructed for $p = 0.3$ and different values of r. The best linear fitting yields the best estimate for the critical value of the parameter r. From the results summarized in Table I (see text), we have located the critical point ($p = 0.3; r = 0.194$).

in Fig. 1 we calculated the goodness of fit Q for the same time interval $[t_1, t_2]$ and obtained the values shown in Table I, from which we obtain the critical value $r = 0.194$.

In order to confirm the critical value obtained in Table I, we have also calculated the critical

TABLE I: Values of Q for different values of r obtained from linear fitting of log-log plots of the magnetization $M(t)$ versus t.

Time interval	r	Q
$[50, 300]$	0.190	2.31×10^{-7}
$[50, 300]$	0.192	0.166
$[50, 600]$	0.194	0.468
$[50, 300]$	0.196	1.04×10^{-28}
$[50, 300]$	0.198	1.09×10^{-76}

value of r for $p = 0.3$ by using the effective exponent, which is given by [21]

$$\lambda(t) = \frac{1}{\Delta t} \log\left(\frac{M(t)}{M(t/\Delta t)}\right). \tag{24}$$

Such exponent takes into account finite-time corrections (finite-time scaling) and, in the limit $t \to \infty$, Eq. (24) behaves as [21]

$$\lambda(t) = c_1 + c_2/t, \tag{25}$$

where c_1 and c_2 are numerical constants and Δt is a fixed time step.

Log-log plots of Eq. (24) are shown in Fig. 2, for $\Delta t = 10$, $p = 0.3$ and $r = 0.190, 0.192, 0.194, 0.196$ and 0.198. From Fig. 2 it is clear that the asymptotic behavior of $\lambda(t)$ given by Eq. (25) is verified for $r = 0.194$, thus confirming the result previously obtained from log-log plots of Eq. (2).

Before presenting the estimates obtained for the critical exponents z and θ_g in the next subsections, it is important to emphasize here that the Monte Carlo simulations were performed only at the critical point ($p = 0.3; r = 0.194$).

B. Critical dynamic exponent z

In order to obtain the dynamic critical exponent z we have perfomed short-time Monte Carlo simulations for square lattices ($d = 2$) with linear dimensions $L = 160$, $N_s = 20000$ samples, $N_b = 5$ sets of samples and 200 MCS. From the definition of the ratio F_2 given by Eq. (5), we have constructed the log-log plot of $F_2(t)$ versus t shown in Fig. 3, obtained from Monte

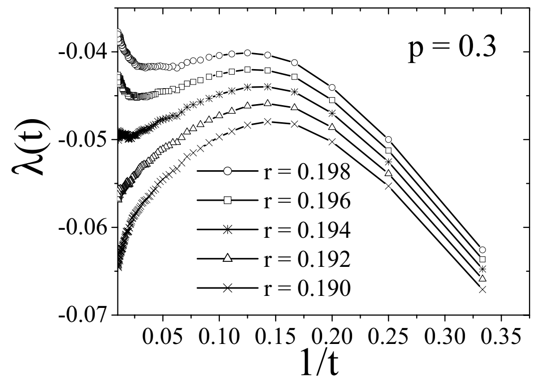

FIG. 2: Effective exponent $\lambda(t)$ obtained for $p = 0.3$ and different values of r. From this graph, we have obtained the critical point ($p = 0.3; r = 0.194$) (See text for details).

Carlo simulations performed for one set of samples. The straight line depicted in Fig. 3 is in accordance with the linear behavior predicted in the scaling relation of Eq. (5).

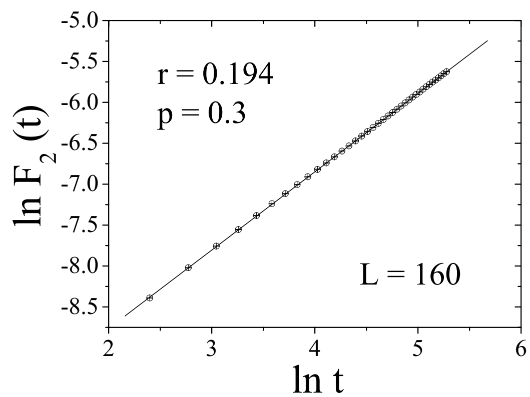

FIG. 3: Typical log-log plot of $F_2(t)$ versus t (straight line), obtained from short-time Monte Carlo simulations at the critical point ($p = 0.3; r = 0.194$).

In Table II we summarize the estimates for z obtained from different time intervals $[t_1, t_2]$, together with the corresponding values of Q.

From Table II, we have obtained the best estimate for the dynamic critical exponent $z = 2.097(8)$, once the goodness of fit $Q = 0.99$ is maximum at the corresponding time interval. However, such value of z is somewhat smaller than $z = 2.17(2)$, which was obtained from the fourth order Binder's cumulant [9]. In order to check the value of z obtained in this work, in the next section we obtain the global persistence exponent from the collapse method, which

TABLE II: Dynamic critical exponent z and the corresponding value of Q obtained for different time intervals.

Time interval	z	Q
$[10, 120]$	2.0853(7)	0.2
$[10, 160]$	2.0856(5)	0.49
$[10, 200]$	2.0869(4)	0.54
$[30, 200]$	2.084(4)	0.98
$[100, 200]$	2.097(8)	0.99

depends on the value of z, and directly from Eq. (20), which does not depend on the value of z. As we shall see in the following, the results for θ_g obtained from these two approaches are in very good agreement with each other.

C. Critical dynamic exponent θ_g

By using Eqs. (21), (22) and (23) given in section III B, we have performed short-time Monte Carlo simulations in order to apply the collapse method of section III B and obtain the dynamic critical exponent θ_g. According with the description of the method, the dynamic exponent z is to be known beforehand. Thus, we have used the value $z = 2.097$ obtained in the previous section. Monte Carlo runs were made up to 1000 MCS for $N_s = 40000$ samples in square lattices with linear dimensions 20, 40 and 80. The collapse method was applied for pairs of linear dimensions $(L_1, L_2) = (20, 40)$ and $(L_1, L_2) = (40, 80)$, from which we have obtained $\theta_g = 0.24(2)$ and $\theta_g = 0.25(2)$, respectively. In Fig. 4 we show the collapse of the curves obtained for $L = 40$ and $L = 80$ with $\theta_g = 0.25$.

Finally, we have obtained the dynamic exponent θ_g directly from the power law predicted in Eq. (20). To this end, we have performed short-time Monte Carlo simulations to obtain the quantity $P(t)$, from which we have constructed log-log curves of $P(t)$ versus t, as depicted in Fig. 5. From Eq. (20), the exponent θ_g was obtained directly from the slope of such curves. Monte Carlo simulations were performed for square lattices with linear dimension $L = 80$ and $N_s = 40000$ samples, where each sample began from the initial state $m_0 = 0.005$. Error bars were estimated from the Monte Carlo runs performed for $N_b = 5$ sets of samples. In Table III we present the results obtained for the exponent θ_g and the corresponding goodness of fit Q for

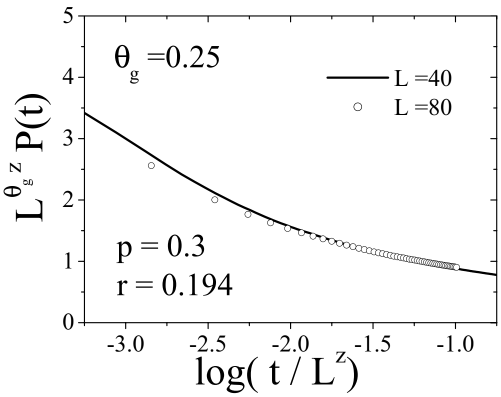

FIG. 4: Collapse obtained from the scaling relation Eq. (21), corresponding to square lattices with linear dimensions $(L_1, L_2 = 40, 80)$ and $\theta_g = 0.25$.

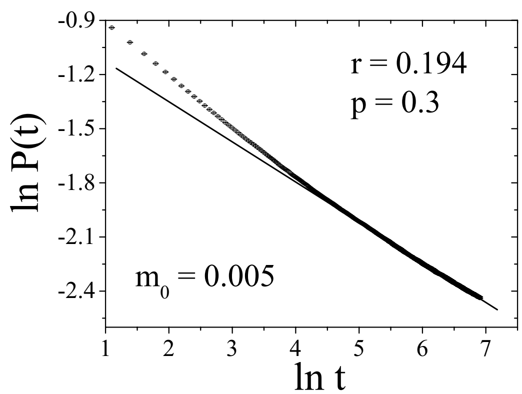

FIG. 5: Typical decay of the probability $P(t)$ (straight line in a log-log plot), obtained from short-time Monte Carlo simulations of $N_s = 40000$ samples with initial state $m_0 = 0.005$.

three different time intervals. From Table III above, the best estimate for the global persistence exponent is $\theta_g = 0.247(4)$, corresponding to $Q = 0.97$. This result is in very good agreement with the estimates $\theta_g = 0.24(2)$ and $\theta_g = 0.25(2)$ obtained from the collapse method.

V. CONCLUSIONS

In this work we have revisited the probabilistic cellular automata proposed by Tomé and Drugowich [6] on the basis of a previous cellular automaton devised by Brass *et al.* [2]. From short-time Monte Carlo simulations, we have obtained the dynamic critical exponent $z = 2.097(8)$ by using a recent technique that mixes different initial conditions [10]. Such result is

TABLE III: Dynamic critical exponent θ_g and the corresponding value of Q obtained for different time intervals.

Time interval	θ_g	Q
$[90, 300]$	0.247(4)	0.97
$[90, 400]$	0.242(3)	0.86
$[100, 500]$	0.238(6)	0.95

slightly smaller than the value $z = 2.17(2)$ obtained from the fourth order Binder's cumulant [9].

We have also performed short-time Monte Carlo simulations in order to obtain estimates for the dynamic critical exponent θ_g, the global persistence exponent, by using two distinct approaches: The collapse method described by Eqs. (21), (22) and (23), and directly from the power law scaling given by Eq. (20). From the collapse method, by using square lattices with linear dimensions $(L_1, L_2) = (20, 40)$ and $(L_1, L_2) = (40, 80)$, we have obtained $\theta_g = 0.24(2)$ and $\theta_g = 0.25(2)$, respectively. Directly from Eq. (20) we have obtained $\theta_g = 0.247(4)$, in very good agreement with the estimates yielded from the collapse method.

Acknowledgments

N. Alves Jr. acknowledges financial support from Brazilian agencies FAPESP and CAPES. R. da Silva thanks GPPD of the Institute of Informatics of Federal University of Rio Grande do Sul (UFRGS), for computational resources.

[1] M. Bezzi. Modeling evolution and immune system by cellular automata. *Riv. Nuovo Cimento*, 24(2):1–50, 2001.

[2] A. Brass, A. J. Bancroft, M. E. Clamp, R. K. Grencis, and K. J. Else. Dynamical and critical behavior of a simple discrete model of the cellular immune system. *Phys. Rev. E*, 50(2):1589–1593, aug 1994.

[3] A. Brass, R. K. Grencis, and K. J. Else. A cellular-automata model for helper t-cell subset polarization in chronic and acute infection. *J. Theor. Biol.*, 166(2):189–200, jan 1994.

[4] R. M. Z. dos Santos and S. Coutinho. Dynamics of HIV infection: A cellular automata approach. *Phys. Rev. Lett.*, 87(16):168102–1–168102–4, oct 2001.

[5] K. J. Else, G. M. Entwistle, and R. K. Grencis. Correlations between worm burden and markers of TH1 and TH2 cell subset induction in an inbred strain of mouse infected with trichuris-muris. *Parasite Immunol.*, 15(10):595–600, oct 1993.

[6] T. Tomé and J. R. Drugowich de Felício. Probabilistic cellular automaton describing a biological immune system. *Phys. Rev. E*, 53(4):3976–3981, apr 1996.

[7] N. R. S. Ortega, C. F. S. Pinheiro, T. Tomé, and J. R. Drugowich de Felício. Critical behavior of a probabilistic cellular automaton describing a biological system. *Phys. Lett. A*, 233:93–98, aug 1997.

[8] G. Grinstein, C. Jayaprakash, and H. Yu. Statistical Mechanics of Probabilistic Cellular Automata. *Phys. Rev. Lett.*, 55(23):2527–2530, dec 1985.

[9] T. Tomé and J. R. Drugowich de Felício. Short-time dynamics of an irreversible probabilistic cellular automaton. *Mod. Phys. Lett. B*, 12(21):873–879, sep 1998.

[10] R. da Silva, N. A. Alves, and J. R. Drugowich de Felício. Mixed initial conditions to estimate the dynamic critical exponent in short-time Monte Carlo simulation. *Phys. Lett. A*, 298:325–329, apr 2002.

[11] H. K. Janssen, B. Schaub, and B. Schmittmann. New universal short-time scaling behavior of critical relaxation processes. *Z. Phys. B*, 73(4):539–549, 1989.

[12] B. Zheng. Monte Carlo simulations of short-time critical dynamics. *Int. J. Mod. Phys. B*, 12(14):1419–1484, jun 1998.

[13] N Alves Jr. and J. R. Drugowich de Felício. Short-time dynamic exponents of an Ising model with competing interactions. *Mod. Phys. Lett. B*, 17(5–6):209–218, mar 2003.

[14] E. Arashiro and J. R. Drugowich de Felício. Short-time critical dynamics of the Baxter-Wu model. *Phys. Rev. E*, 67(4):046123, apr 2003.

[15] R. da Silva, N. A. Alves, and J. R. Drugowich de Felício. Universality and scaling study of the critical behavior of the two-dimensional Blume-Capel model in short-time dynamics. *Phys. Rev. E*, 66(2):026130, aug 2002.

[16] N Alves Jr. and J. R. Drugowich de Felício. Short-time critical dynamics at the Lifshitz point of the ANNNI model. , to be published.

[17] R. da Silva, J. R. Drugowich de Felício, and R. Dickman. , cond-mat/0404065.

[18] S. N. Majumdar, A. J. Bray, S. J. Cornell, and C. Sire. Global Persistence Exponent for Nonequilibrium Critical Dynamics. *Phys. Rev. Lett.*, 77(18):3704–3707, oct 1996.

[19] S. Wolfram. Statistical-Mechanics of Cellular Automata. *Rev. Mod. Phys.*, 55(3):601–644, 1983.

[20] R. da Silva, N. A. Alves, and J. R. Drugowich de Felício. Global Persistence Exponent of the Two-Dimensional Blume-Capel Model. *Phys. Rev. E*, 67(5):057102, may 2002.

[21] P. Grassberger and Y. Zhang. "Self-organized" formulation of standard percolation phenomena. *Physica A*, 224(1–2):169–179, feb 1996.